

# Extreme paleoflood events 3200–3000 a BP in the Jingyuan–Jingtai reaches of the upper Yellow River, China

The Holocene  
1–11  
© The Author(s) 2016  
Reprints and permissions:  
sagepub.co.uk/journalsPermissions.nav  
DOI: 10.1177/0959683615618257  
hol.sagepub.com  


**Guiming Hu, Chun Chang Huang, Yali Zhou, Jiangli Pang,  
Xiaochun Zha, Yongqiang Guo, Yuzhu Zhang and Xueru Zhao**

## Abstract

A set of paleoflood slack water deposit (SWD) beds was identified within slope clasts at the Jinpingcun (JPC) site in the Jingyuan–Jingtai reaches of the upper Yellow River gorges based on sedimentary criteria and analytical results. Paleoflood hydrology methods were applied to reconstruct paleoflood events in the Jingyuan–Jingtai reaches. The paleoflood peak stages were calculated based on the highest end-point elevations of the SWDs. The HEC-RAS model and optically stimulated luminescence dating enabled robust paleo-discharge estimates to be calculated between 12,750 and 16,310 m<sup>3</sup>/s for paleoflood events that occurred during 3200–3000 a BP. The peak discharges, including gauged and historical flood data at the Lanzhou gauge station and the reconstructed paleoflood peak discharges at the JPC site, were input for flood frequency analysis. These paleo-hydrological approaches can also be applied to other regions in the Yellow River gorges. Furthermore, the ages of the paleoflood events correspond well with the known climatic events at 3100 a BP during Holocene climatic variability. These findings are significant for flood risk estimation, in the assessment of water sources in dryland environments, and in understanding the interactions between hydrological systems and climatic change in arid and semi-arid regions of the upper Yellow River in China.

## Keywords

China, climatic change, HEC-RAS model, paleoflood hydrology, slack water deposit, upper Yellow River

Received 14 May 2015; revised manuscript accepted 22 October 2015

## Introduction

In recent years, several flood events and flood damages on the upper Yellow River have been reported in the mass media and have caused direct economic losses up to several billion dollars and human casualties (e.g. floods in 1981, 2005, and 2009). Global climate change has exerted significant impacts on the fluvial system, where temperature changes and extreme precipitation events can occur (Milly et al., 2008). Kang et al. (2015) applied hydrological and regional climate models to simulate future climate and hydrologic changes over the Yellow River basin. The simulation results predict that river runoff in the upper Yellow River basin will increase by 6.4% from 2019 to 2048. In northern China, the East Asia monsoon will be characterized by high seasonal variability because of global warming and the climatic characteristics will result in more precipitation and flood disasters during the 21st century (Huang and Du, 2010). However, because credible past flood information is missing, it is still urgent for the science community to address the ancient flood risk and difficult for stakeholders and policy-makers to provide informed decision-making. For the government to improve present assessments of how future hydroclimatic systems will affect society, scientific research on the relationships between paleofloods and climatic change on millennial, or longer, timescales is urgently needed (Støren et al., 2012).

Slack water deposits (SWDs) are coarse-grained sediments conveyed in suspension during highly energetic flood flows that are deposited in areas of flow separation that result in long-term

preservation after flood recession (Baker et al., 1983). The common materials applied worldwide to infer paleoflood parameters involve SWD-paleostage indicators (SWD-PSIs) and lake sediment cores (Baker, 1987; Wirth et al., 2013; Sheffer et al., 2008). These indicators have been used in an effort to reconstruct paleoflood events during the Holocene (e.g. Baker, 1987, 2006; Baker et al., 1983, Benito et al., 2003, 2004; Benito and Thorndycraft, 2005; Ely and Baker, 1985; Thorndycraft et al., 2005). Compared with other dating techniques, the chronology of extreme paleoflood events is preferably determined using the pedo-stratigraphic correlation, C<sup>14</sup>, and optically stimulated luminescence (OSL) dating (Kochel and Baker, 1982; Rittenour et al., 2003; Thomas et al., 2005). If the SWDs are interbedded in the Holocene eolian loess-soil profiles, the pedo-stratigraphic correlation may be a suitable method (e.g. Huang et al., 2011, 2012a, 2012b, 2013). In the Jinpingcun (JPC) profile, the SWDs are not markedly affected by weathering and pedogenesis after deposition, and no wood, charcoal, or animal bones were found in the SWD bedsets.

---

Department of Geography, Shaanxi Normal University, P.R. China

## Corresponding author:

Chun Chang Huang, Department of Geography, Shaanxi Normal University, Xi'an, Shaanxi 710062, P.R. China.  
Email: cchuang@snnu.edu.cn

Therefore,  $C^{14}$  dating was not used to determine the chronology in the JPC profile. The OSL dating method has been successfully applied to dating fluvial deposits in recent years (Galbraith, 1990; Rittenour et al., 2003; Thomas et al., 2005; Zhang et al., 2003). Therefore, the OSL dating technique was selected to determine the chronology of the extreme paleoflood events at the JPC site. The paleoflood peak stages and peak discharges were calculated using hydraulic methods and models.

The upper Yellow River basin is a region sensitive to global climate change (Xie et al., 2011), and it has experienced intense neotectonic activities. In addition, human activities, including overplanting and grazing, heavy plant harvest, and poor watershed management, have destroyed the ground surface and landforms in the region. These factors have resulted in many geological disasters, for example, earthquakes, landslides and debris flows, and land desertification. The upper Yellow River basin drains through arid and semi-arid regions in China. The mean discharge of the upper Yellow River at the Lanzhou gauge station is  $1040 \text{ m}^3/\text{s}$ . The mean annual temperature varies from  $-5$  to  $9.7^\circ\text{C}$ , and the mean annual precipitation varies from 370 to 600 mm (Ren and Feng, 2008). Because of the arid climate, the exploitation and use of water resources have become increasingly significant for the region. The reconstruction of paleoflood hydrology is therefore necessary and essential for both water-resource management and flood risk planning in this region. However, little has been reported on the paleo-hydrological investigation of the upper Yellow River basin (Li, 2013). During paleo-hydrological, sedimentary, and geomorphological fieldwork in the upper stream of the Yellow River, one episode of 14 extreme flood events was identified at the JPC site in Jingyuan County. These are the result of river systems responding to rapid or abrupt climatic change during 3200–3000 a BP, which was defined by dry–cold periods (Mayewski et al., 2004). In the study region, the climate shows a continued drying trend during the late Holocene, which is likely in response to an abnormal change in the East Asian monsoon (COHMAP, 1988). Based on studies of loess/paleosol (Lo/So) over the middle reaches of the Yellow River, the pedogenic regression in Lo was forced by intensified aridity, dust storms, and dust falls in connection with monsoonal climatic shift during the late Holocene from 3100 a BP to the present (Huang et al., 2009, 2012a, 2012b). Significant climatic dry–cool episodes were also documented at around 3100 a BP in studies of lake sediments from the middle Yellow River basin and the adjacent arid to semi-arid regions (Chen et al., 2003; Peng et al., 2005; Shi et al., 1992; Sun and Zhao, 1991; Xiao et al., 2004, 2009).

The main objectives of this paper are (1) to identify Holocene extreme paleoflood events using the sedimentological criteria established by Huang et al. (2011, 2012a, 2012b, 2013), (2) to establish the chronology of these paleoflood events using the OSL dating method, and (3) to reconstruct the peak flood stages and discharges using the HEC-RAS hydraulic model (US Army Corps of Engineers Hydraulic Engineering Center, 2010).

## Study area and site

The mainstream of the Yellow River is 5464 km in length and drains an area of  $752,000 \text{ km}^2$  (Figure 1a and b). Large parts of the river basin belong to the monsoonal climate region (Figure 1c). From its headwaters in Hekou Town (Togtoh County, Inner Mongolia Autonomous Region), the upper reaches of the Yellow River drain a catchment area of  $386,000 \text{ km}^2$  and are 3471.6 km in length. The upper reaches of the mainstream from the headwaters to Madu flow through the Tibetan Plateau, from the Jishi gorge to the study site (Figure 2a) through the Loess Plateau. The upper reach experiences a dry climate, with an annual mean temperature range of  $-5$  to  $9.7^\circ\text{C}$  (Ren and Feng, 2008). The mean annual precipitation in

the river basin is 466 mm, and rainstorms are intense and often occur in the summer. The upper mainstream is characterized by many meanders and deep canyons. The flood waters are mainly composed of large and continuous rainfall, with additional snow-melt. The seasonal changes of flooding match that of the rainfall, occurring between June and October (Gao et al., 2002).

Since the Mid-Pleistocene Epoch, the Yellow River has cut into metamorphic rocks along the reaches from the Jingyuan to Jingtai county, forming a stable and narrow valley (Liu and Wang, 2002; Ran et al., 2009; Zhang et al., 2008). Patches of well-rounded gravels are deposited at the confluences where the tributaries join the mainstream. The study reaches are bedrock-influenced and the channel is confined by the canyon along two sides (Figure 2a and b). The river flowed through the pedestal terrace and cut into metamorphic rocks. Based on previous studies, this channel form has remained relatively unchanged during the Holocene (Zhang et al., 2008). The JPC site (Figures 1b and 2a) is located in Jinpingcun Village, on the northern side of Jingyuan County. Modern villages are situated at the first river terrace that is 20–30 m higher than the present normal water level. The northern bank of the Yellow River at the JPC site is exposed bedrock cliffs. The southern bank has Jinpingcun Village, farmlands, and orchards. The southern side has gentle slopes with slope clasts overlapping the basement of the bedrock. At the JPC site, a set of paleoflood SWDs was identified interbedded in the slope deposits in the roadcut of the southern bank. The top of the JPC profile is 1312 m higher than the present normal water level of 17 m. The bottom of the profile is 1307 m a.s.l. and overbank flood events exceeding this elevation have left physical evidence.

## Methods

### Paleoflood analysis

Paleoflood SWDs are the direct sedimentary evidence of paleoflood events in riverbanks and are critical for reconstructing the peak flood stages and discharges. In the field, the SWD bedsets are often buried and preserved by various surface processes. Therefore, using physicochemical characteristics (e.g. particle-size distribution and magnetic susceptibility) and the sedimentological criteria to distinguish the paleoflood SWDs from other deposits (e.g. Holocene loess and paleosol, slope deposits) is important for paleo-hydrological study. The sedimentological criteria used for the identification of paleoflood SWDs include (1) sediments consisting of silt, clay silt, sandy silt, and silty sand, forming parallel, sloping, or waving beddings; (2) abrupt vertical change in particle size, color, texture, and structure; (3) sorted deposition with fine sand at the bottom and clay cap at the top, with stratigraphic breaks between the beds; (4) mud cracks in clay and clayey silt beds, forming enterolithic structures in the profile; and (5) depositional discontinuity between two flood events, with insertion of slope wash and clasts, loess, paleosol, eolian sand, tributary coarse-sized alluvium, bioturbation, and anthropogenic remains (Benito et al., 2004; Benito and Thorndycraft, 2005; Huang et al., 2013; Kale et al., 2000; Sheffer et al., 2008; Sridhar, 2007; Thorndycraft et al., 2005). After detailed observations in the field, eight sedimentology samples for particle-size distribution and magnetic susceptibility, and three samples for OSL dating, were taken from the JPC profile. The 2012 flood SWD in the same reach was used for comparison with the paleoflood SWDs in physicochemical properties. Magnetic susceptibility was measured on a mass of 10 g of ground sediment with a Bartington MS2 magnetic susceptibility meter (0.47/4.7 kHz). The particle-size distribution of the samples was determined using a Backman Coulter-LS laser analyzer with  $(\text{NaPO}_3)_6$  as a dispersing agent after pretreatment with 30%  $\text{H}_2\text{O}_2$  to remove organic material and

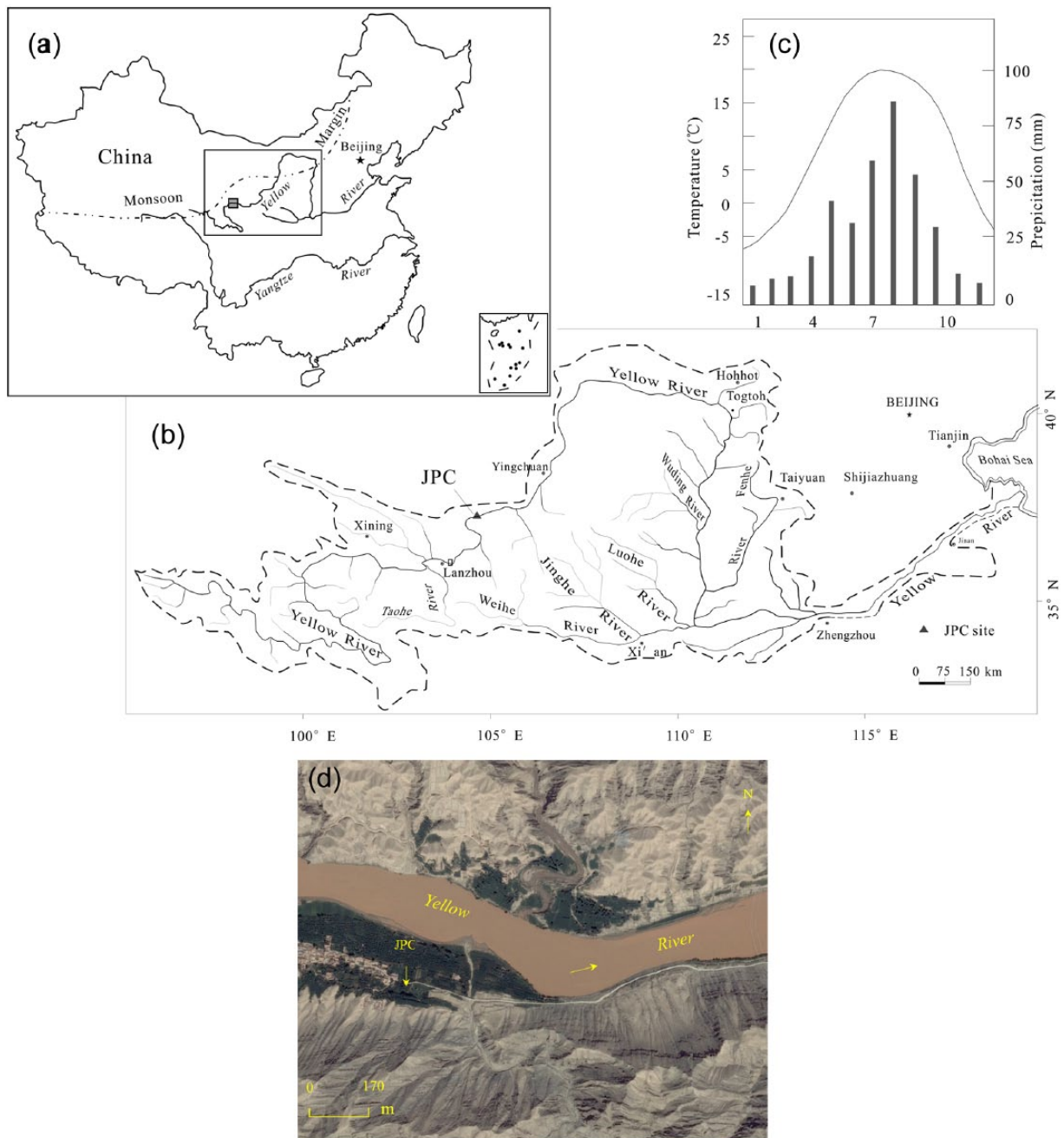


**Figure 1.** (a) An inset map showing the study reach and correlated regions marked by a rectangle in the Yellow River in China. The gray square indicates the study river reach on the Yellow River. The black dotted line indicates the boundary between monsoon and non-monsoon regions in China. (b) Site map showing the Yellow River drainage basin and the location of the Weihe and Jinghe rivers on the Yellow River. The study site, Jinpingcun (JPC), on the upper Yellow River is marked by the gray triangle. The Lanzhou gauge station is indicated with a rectangle near Lanzhou City. (c) The annual figure for temperature and precipitation in Lanzhou City, Gansu Province, China. (d) Satellite image showing the landscape of the bedrock gorge.

10% HCl to dissolve carbonates. The analytical results are presented in the 'Results' section.

#### OSL dating of the paleoflood events

OSL dating on the fine sands fraction (125–180  $\mu\text{m}$ ) of polyminerals was carried out using the double single-aliquot regenerative-dose (SAR) protocol (Banerjee et al., 2001; Murray and Wintle, 2000) in the TL/OSL Dating Laboratory at Shaanxi Normal University. All the measurements were performed on a Risø-TL/OSL-DA-20 dating system equipped with a combined blue (470 nm, 50 mW/cm<sup>2</sup>) and infrared (875 nm, 150 mW/cm<sup>2</sup>) LED unit coupled with a <sup>90</sup>Sr/<sup>90</sup>Y beta source irradiation (Bøtter-Jensen and Duller, 1992). The concentrations of uranium (U), thorium (Th), and potassium (K) in the samples were determined by

neutron activation analysis in the China Institute of Atomic Energy in Beijing, and the effective dose rate ( $D_y$ ) was calculated from the elemental concentrations using the revised dose-rate conversion factors (Adamiec and Aitken, 1998). The water content of the collected flood SWDs was measured after drying at 105°C for 12 h. The OSL dates were calculated using the computer program Age.exe (Grün, 2003).

#### Application of HEC-RAS modeling

The estimation of paleoflood discharges using the step-backwater method was performed with the HEC-RAS Version 4.1.0 of US Army Corps of Engineers River Analysis System and ArcGIS Environment (US Army Corps of Engineers Hydraulic Engineering Center, 2010; Webb and Jarrett, 2002). The HEC-RAS

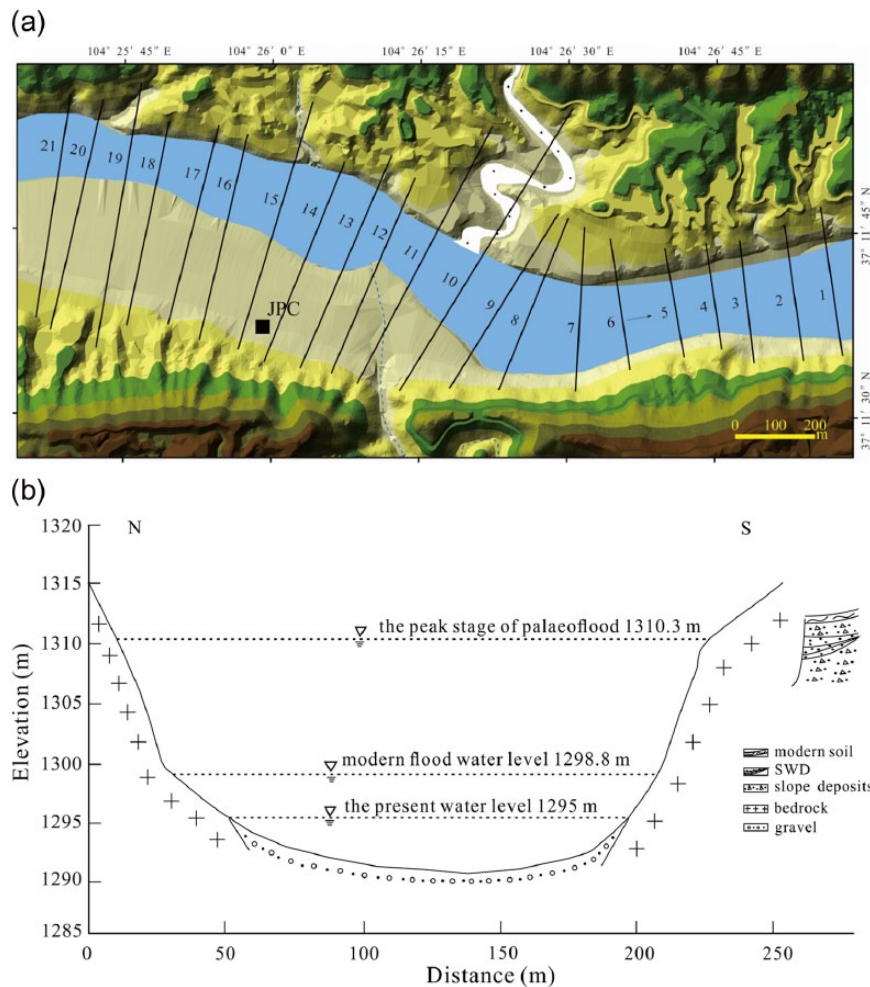


**Figure 2.** (a) Map showing the topography of the surveyed cross-sections at the JPC site in the upper Yellow River gorges and the location of the study site, JPC, marked with a black square. (b) Cross-section 4 of the paleo-hydrological reconstruction at the JPC site on the Yellow River channel, showing the lithology of the upper Yellow River at the JPC site.

software allows one-dimensional steady and unsteady flow river hydraulics calculations. The computation procedure is based on the solution of the one-dimensional energy equation, derived from the Bernoulli equation, for steady gradually varied flow (O'Connor and Webb, 1988). The natural channels have almost unsteady and non-uniform flow; however, the channel geometry in the studied reach has no major changes, so one can assume it is steady varied gradual flow. The accuracy of the discharge estimations depends on the cross-section stability. In the studied reach, the channel geometry at the maximum of the stable, bedrock-confined channels is known to have had no (or approximately no) major changes during the Holocene (Liu and Wang, 2002; Ran et al., 2009; Zhang et al., 2008). According to the flow regime and flow form, the contraction and expansion of the channel are not abrupt in the study channel. Therefore, the values of contraction and expansion were selected as 0.1 and 0.3 (US Army Corps of Engineers HEC, 2010), respectively. The channel slope is usually expressed as a gradient, which is related to the water-surface slope and downstream change in the water-surface elevation along the channel. Furthermore, because the water-surface slope closely approximates the energy slope along a particular length of channel, the energy slope of the study reach can be replaced by the channel slope referring to the HEC-RAS v4.1 Reference Manual. The unsteady, gradually varied flow in most natural channels is subcritical, as in the study channel ( $Froude < 1$ ). This means that there is no obvious hydraulic jump or hydraulic drop on the channel bottom. This fluvial geomorphic setting satisfies the requirements of the HEC-RAS model in this

channel. A total of 21 cross-sections were surveyed at a river channel approximately 2.2 km in length, and at a distance of between 80 and 100 m apart, calibrating from the 1:10,000 scale map to set up a normal depth boundary condition ( $S=0.0012$ ) at the starting cross-section. The river channel topography was obtained by direct measurements of water depth, using a graduated rod operated from a boat and taking a rope fixed at both sides of the river as a reference position.

## Results

### *Sedimentary characteristics of the fluvial deposits*

During the field investigation, a set of paleoflood SWDs with waving and slope bedding was identified based on sedimentary criteria and physicochemical properties. The features were preserved on the roadcut of the southern bankside at the JPC site (Figure 2a). The yellow–orange paleoflood SWDs and the gray slope deposits are clearly visible at 3.0 m thick. The individual bed was deposited by a single overbank flooding event and there was discontinuity between each one by distinct stratigraphic breaks (Figure 3). The sedimentary characteristics and pedo-stratigraphic subdivisions of the JPC profile are shown in Figure 4.

The particle-size distribution at the JPC site is shown in Table 1. The SWD contains mostly coarse silt (67.89–86.80%), followed by fine silt (3.10–31.60%) and clay (4.94–10.1%),



**Figure 3.** Photo of the paleoflood SWD in the Holocene sediment profile at the JPC site along the upper Yellow River.

similar to the modern flood deposit (79.75%, 13.80%, and 4.95%, respectively). Otherwise, the indexes of  $M_d$ ,  $M_z$ ,  $O$ ,  $S$ , and  $K_g$  in the paleoflood SWDs are similar to the modern flood deposit, characteristic of fluvial deposits. The particle-size curves are shown in Figure 5. The peak curves of SWDs at the JPC site are 22.73–47.94  $\mu\text{m}$ . The distribution is therefore concentrated relatively. In particular, the peak is single and narrow, especially for SWD1 and SWD5, which is similar to SWD2012 (33.01–43.67). Based on an integration of the field investigations and analytical results in particular, by a comparison with that of the 2012 flood SWD in the same reach, the fluvial bedsets are identified as typical paleoflood SWDs and they are the physical evidence of paleoflood events.

**Peak stages and discharge estimation of flood events**

Based on field observations, satellite images (Figure 1d), human activities, and referring to the Hydrological Calculation Norms for Hydraulic Engineering in China, the assigned Manning’s  $n$  values varied between 0.035 and 0.060. A single flood event can

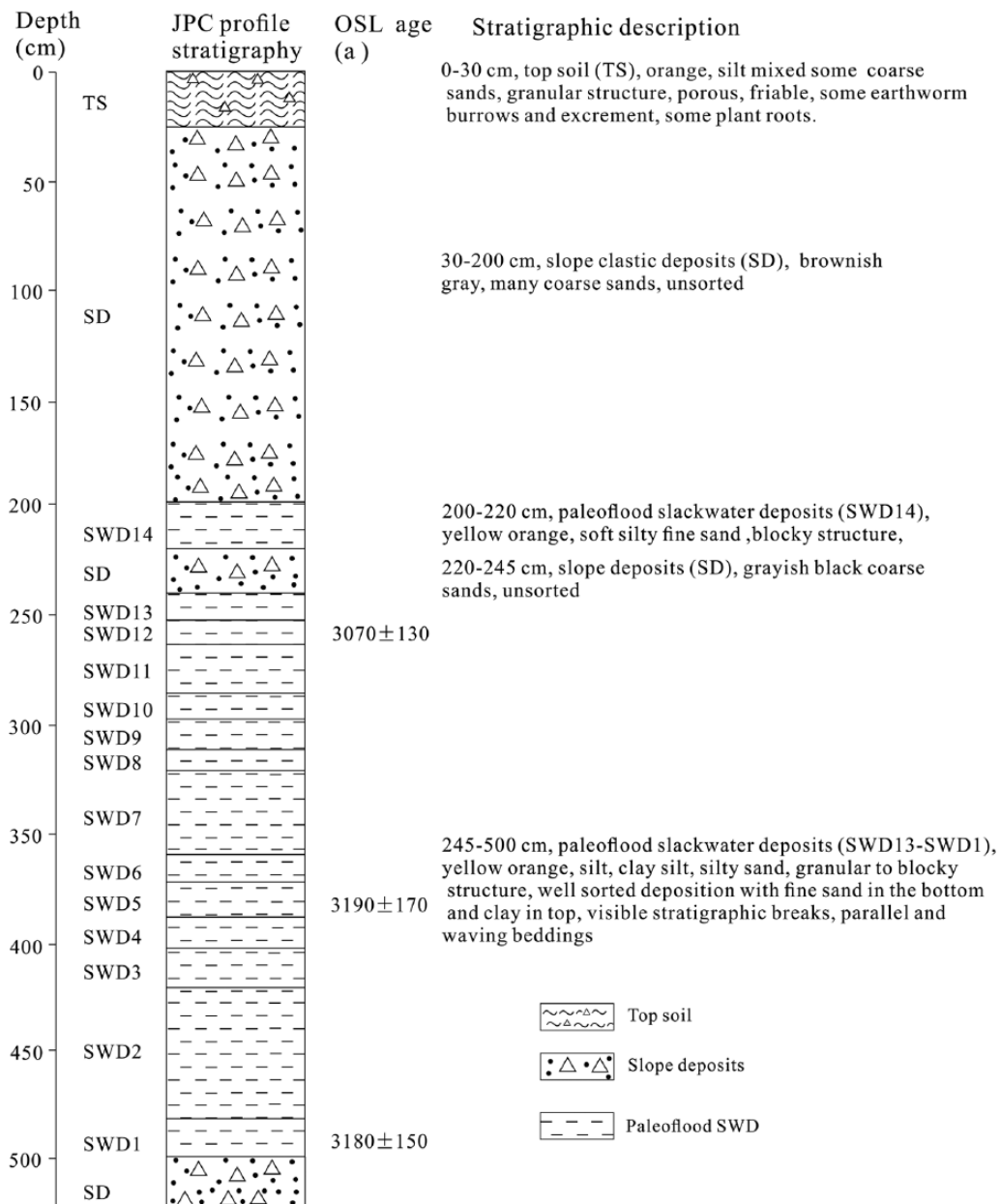


**Figure 4.** Stratigraphic subdivisions and descriptions of the top soil, paleoflood SWD, and slope clasts at the JPC site along the Jingyuan–Jingtai reach in the upper Yellow River.

**Table 1.** Magnetic susceptibility and particle-size distribution of the Holocene paleoflood SWD, 2012 flood SWD at the Jinpingcun site along the upper Yellow River.

Sediment	Magnetic susceptibility ( $\times 10^{-8} \text{ m}^3/\text{kg}$ )	Particle size (%)					Md ( $\mu\text{m}$ )	Mz ( $\mu\text{m}$ )	$\Delta$	SK	Kg	S
		<2 $\mu\text{m}$	2–16 $\mu\text{m}$	16–63 $\mu\text{m}$	63–125 $\mu\text{m}$	>125 $\mu\text{m}$						
SWD12	21.9	10.1	45.6	41.20	3.00	0.10	13.81	16.41	1.69	0.30	1.11	1.07
SWD11	25.3	6.86	27.94	55.00	8.70	1.50	23.72	26.76	1.66	0.33	1.34	0.92
SWD7	35.7	5.23	16.97	53.10	20.30	4.40	38.14	45.25	1.65	0.37	1.40	0.88
SWD5	30	4.94	12.76	57.00	24.10	1.20	42.63	43.96	1.47	0.44	1.66	0.69
SWD2	26.8	6.45	25.95	54.20	11.30	2.10	26.00	31.08	1.69	0.32	1.29	0.96
SWD1	31.8	4.91	11.49	56.40	23.90	3.30	44.51	45.99	1.46	0.42	1.78	0.66
2012 Flood SWD	39	4.95	13.75	66.00	13.80	1.50	35.59	39.97	1.39	0.39	1.74	0.65

SWD: slack water deposit.

The curves of particle size distribution of paleoflood and 2012 flood SWD

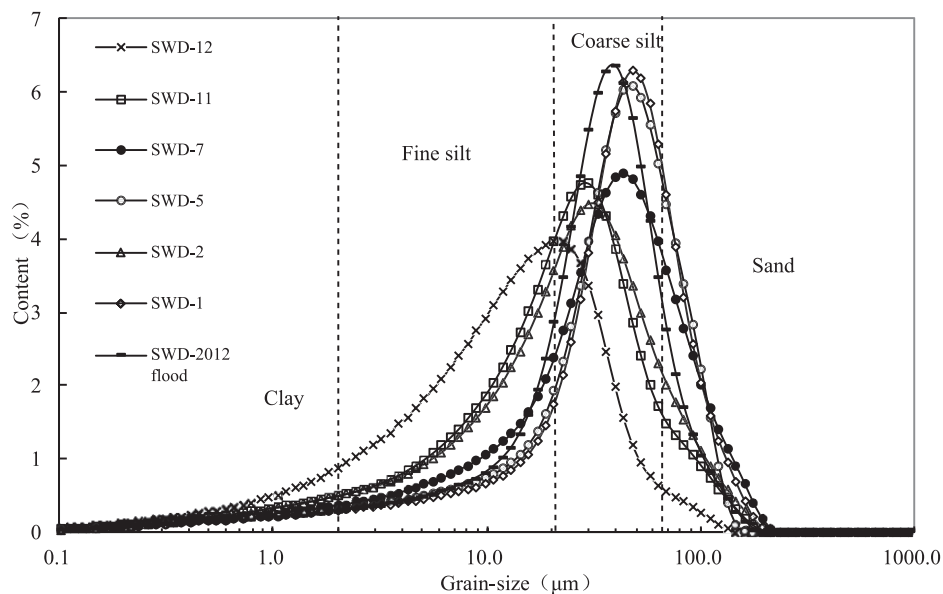


**Figure 5.** Curves showing particle-size distribution frequency of the paleoflood SWD in comparison with that of the 2012 flood SWD at the JPC site in the upper Yellow River.

leave its highest end-point, an indication of the minimum peak stage of the paleoflood events (Benito et al., 2004; Yang et al., 2000). The elevations of modern flood and paleoflood SWD end-points were acquired during fieldwork (Table 2). Along with other hydraulic parameters, Figure 6 shows the reconstructed water-profiles along the Jingyuan–Jingtai reaches of the paleoflood, modern flood, and the present water level using the HEC-RAS model and ArcGIS. The 21 cross-sections, with 80–100 m between each one, in the channel and the highest peak stage of the floods are presented in Figure 6 and Table 2. The estimated paleoflood peak discharge of these ancient flood events is calculated to be between 12,750 and 16,310  $\text{m}^3/\text{s}$ .

A sensitivity test performed on the hydraulic calculations shows that for a 25% variation in Manning's  $n$  values ( $0.75n$  and  $1.25n$ ), an error of 5–10% will be introduced into the estimated discharges (Table 2) at the cross-sections of the river channel matching the end-points of the modern flood and paleoflood SWD. Furthermore, the discharge of SWD14 using the surveyed end-point elevation varies between 15,000 and 17,800  $\text{m}^3/\text{s}$ , and an error of up to 8% may be introduced into the discharge results because of roughness coefficient uncertainties in cross-section 4. Uncertainties in Manning's  $n$  values and energy loss coefficients had much less impact than uncertainties in cross-section data on discharge values estimated from hydraulic modeling (O'Connor and Webb, 1988).

The large 2012 flood peak discharge was gauged as 2960  $\text{m}^3/\text{s}$  at the Jingyuan reach. The physical evidence of the 2012 flood along the reach can be used to calibrate the HEC-RAS model. For the selected Manning's  $n$  and energy loss coefficients, the peak discharge of the 2012 flood event was reconstructed as 2730–3220  $\text{m}^3/\text{s}$  (Table 2). Furthermore, the rating curves in cross-section 4 show that the estimated discharges of paleoflood SWD14 vary between 15,000 and 17,800  $\text{m}^3/\text{s}$  (Figure 7). The reconstructed and gauged discharge of 16,310 and 2960  $\text{m}^3/\text{s}$ , respectively, fall well into the estimated range of discharges, which suggests that the reconstructed paleoflood peak discharges with the HEC-RAS model are reliable.

## Discussion

### Hydrological techniques and their applied conditions

The paleoflood SWD was identified based on sedimentological criteria and laboratory analysis. The hydrological parameters (e.g. river channel topography, cross-sections, and flood deposit elevations) were acquired during fieldwork. The minimum paleoflood peak stages were used as the elevation of the SWD end-points and the minimum paleoflood peak discharges were estimated from HEC-RAS hydraulic modeling and ArcGIS. The method is based on the step-backwater calculations (Webb and

**Table 2.** Paleoflood peak stages, 2012 flood and normal water level, and results of the sensitivity test performed on the hydraulic calculations in the Jingyuan–Jingtai reach of the upper Yellow River.

Paleoflood	Stage (m a.s.l.)	Q (m <sup>3</sup> /s)			Variation (%)	
		$n \times 1.25$	$n \times 1$	$n \times 0.75$	$n \times 1.25$	$n \times 0.75$
JPC-SWD1	1308	11,520	12,750	13,540	-9.64	6.20
JPC-SWD2	1308.9	12,910	14,350	15,120	-10.03	5.37
JPC-SWD7	1309.6	13,670	15,110	16,080	-9.53	6.50
JPC-SWD11	1309.7	13,840	15,300	16,250	-9.54	6.20
JPC-SWD14	1310.3	14,630	16,310	17,250	-10.30	5.80
Normal water level	1295	910	1010	1070	-9.90	5.92
2012 flood	1298.8	2730	3040	3220	-10.20	5.94

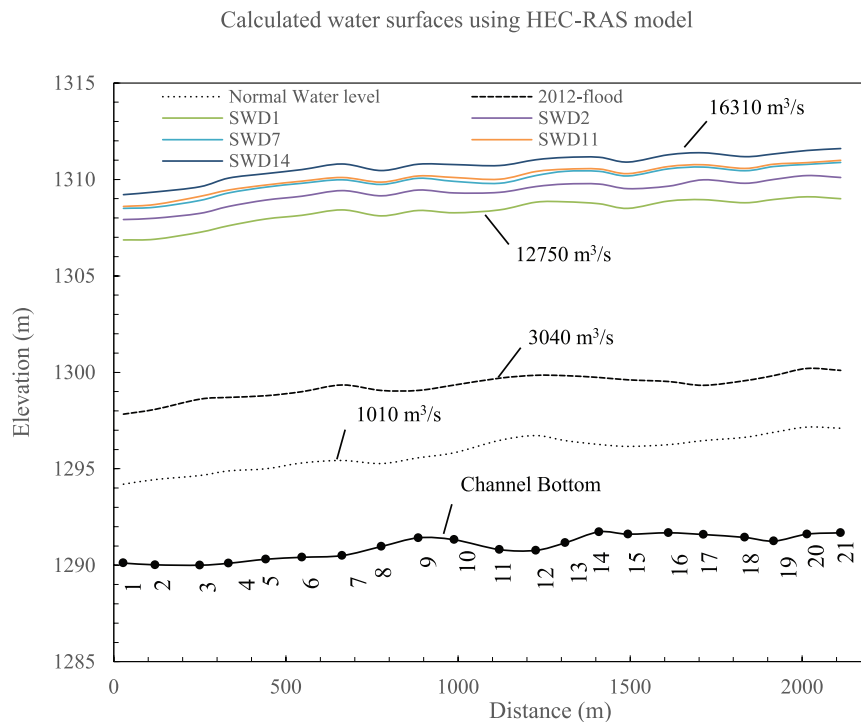


**Figure 6.** Calculated water-surface profiles of the paleoflood, the 2012 flood, and normal water level.

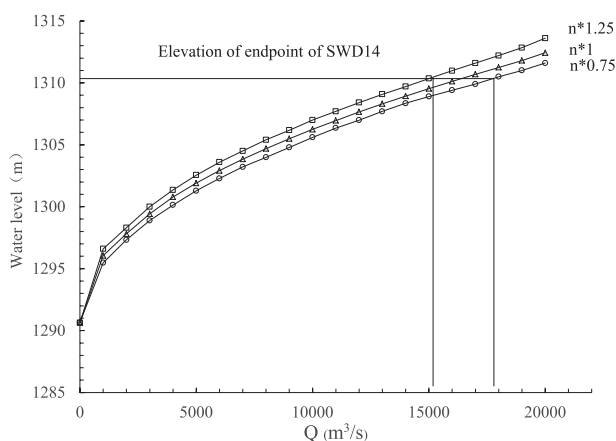


**Figure 7.** Rating curves of cross-section 4 in the Jingyuan–Jingtai river reach. Manning's  $n$  values were assigned for the 25% variation. The results show that the discharges of SWD14 vary between 15,000 and 17,800 m<sup>3</sup>/s.

Jarrett, 2002). The paleo-hydrological techniques that apply to the wider river reach of the Yellow River basin must satisfy the following criteria: (1) the flood flow was subcritical and varied

gradually along the modeling river reach in the Yellow River for the application of the HEC-RAS model, (2) the typical Holocene paleoflood SWD profile can be identified from other deposits in the various earth surface processes according to the sedimentary criteria and analytical laboratory results, (3) the stratigraphic breaks are clearly visible and the elevation of end-points is clearly investigated, and (4) the highest end-point of the modern large flood SWD was left on the studied river reach and was also surveyed for calibrating the reliability of paleoflood peak discharges reconstructed using HEC-RAS hydraulic modeling.

#### Implications of the paleo-hydrological study

The Lanzhou gauge station in the upstream is 200 km away from the JPC site (Figure 1b). Since 1934, the largest gauged flood with discharges was 5600 m<sup>3</sup>/s, recorded on 15 September 1981, and the largest historical flood with discharges was 8500 m<sup>3</sup>/s, recorded on 17–18 July 1904 (Liu and Wang, 2002) (Figure 8b). However, the longer term perspective in the study area, on a millennial-scale or more, on flood frequency and magnitude, is difficult to analyze. Based on the investigation of paleoflood events in the Jingyuan–Jingtai reach of the upper Yellow River, five paleoflood peak discharges were reconstructed based on the paleo-hydrological method (Table 2). The improvement in the

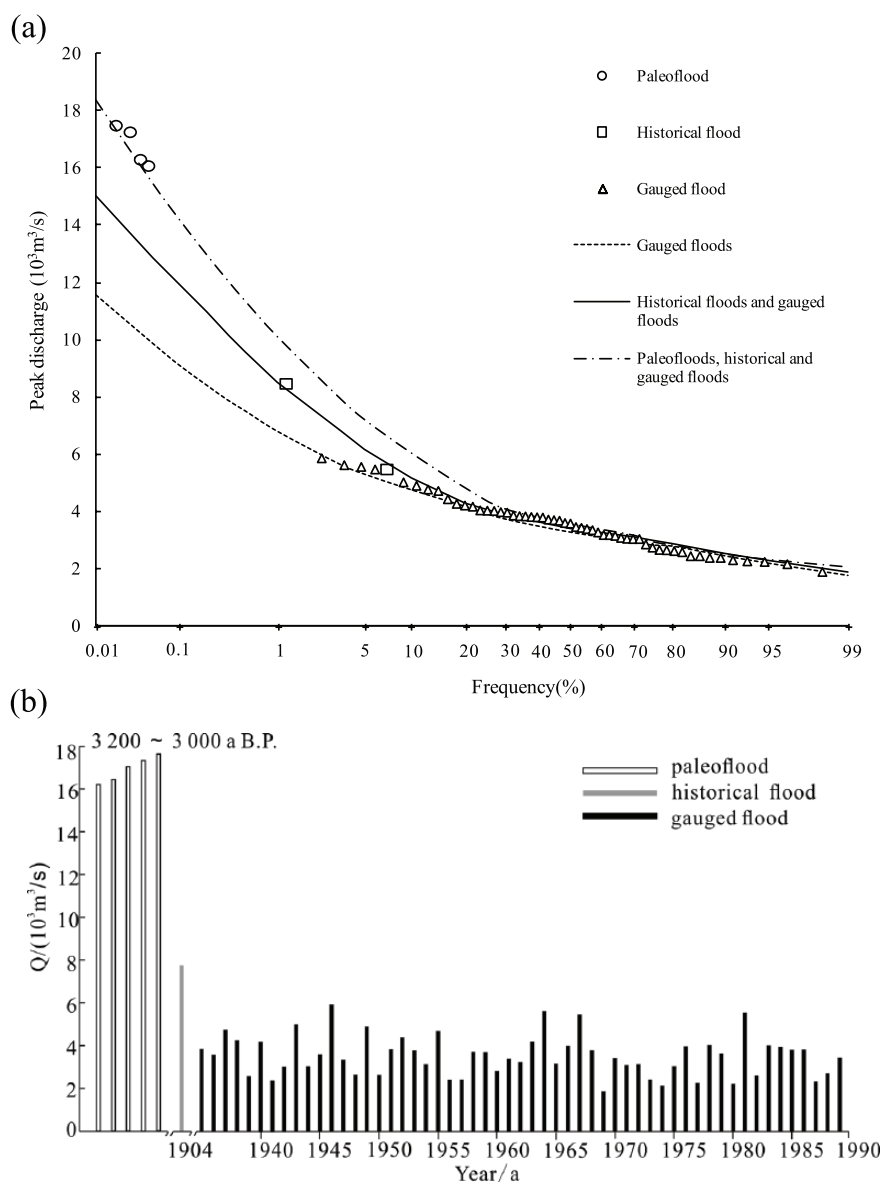


**Figure 8.** (a) Flood frequency–peak discharge relationship curve established with a combination of gauged flood (1934–1989), historical flood (1904 and 1935), and paleoflood data at the Lanzhou gauged station in the upper Yellow River. (b) Non-systematic flood data at the Lanzhou hydrological station in the upper Yellow River basin.

**Table 3.** Summary of the dosimetry, equivalent dose, and OSL ages in the JPC profile on the upper Yellow River valley.

Sample	Depth (cm)	U (ppm)	Th (ppm)	K (%)	Water (%)	De (Gy)	Dy (Ga/ka)	Age (a)
SWD1	470	2.46 ± 0.10	10.3 ± 0.30	1.93 ± 0.06	12.8	9.81 ± 0.39	3.08 ± 0.07	3180 ± 150
SWD5	370	2.56 ± 0.10	9.85 ± 0.30	1.75 ± 0.06	12.6	8.99 ± 0.43	2.82 ± 0.61	3190 ± 170
SWD12	260	3.10 ± 0.12	11.1 ± 0.31	2.07 ± 0.06	12.6	10.13 ± 0.38	3.31 ± 0.63	3070 ± 130

frequency curve estimation was made using gauged flood data from 1934 to 1989, historical floods of 1904 and 1935 at the Lanzhou gauged station, and Holocene paleoflood discharges available in the upper Yellow River (Figure 8a). From the frequency plot in Figure 8a, it is clear that the discharge of the 1000-year return-period at the Lanzhou gauged station is 14,200 m<sup>3</sup>/s and for the 10,000-year return-period is 18,400 m<sup>3</sup>/s based on the paleoflood, historical, and gauged data. Furthermore, based on the results of the flood events, the paleoflood events during 3200–3000 a BP at the JPC site were the largest ever recorded to have occurred in the upper Yellow River during the Holocene. These results not only prolong the time series of floods but are also important for flood hazard mitigation.

The upper Yellow River basin is located in a semi-arid to arid region with a fragile environment and is very sensitive to monsoonal climatic change. Global climate change may induce increased social vulnerability to flood risks in these regions. Studies of the occurrence of large, modern flood events in the upper Yellow River are usually related to the abnormal monsoonal atmospheric pattern (e.g. 1999, 2002 and 2012 flood; La et al., 2013; Lan et al., 2007). Similarly, studies of Holocene paleoflood events and the associated climatic patterns will not only increase our understanding of the effects of global and regional climatic change on the fluvial system environment but also provide information used to interpret and calibrate the modern short-term gauged records.

The age of the paleoflood depositional episode at the JPC site in the upper Yellow River basin was determined by OSL dating (Table 3). The OSL dating samples from paleoflood SWDs 1, 5, and 12 were obtained from the JPC profile and were dated to  $3180 \pm 150$  a BP,  $3190 \pm 170$  a BP, and  $3070 \pm 130$  a BP, respectively, corresponding well to the phase of global climatic declines and variability during the Holocene (e.g. Bond et al., 2001; Haug et al., 2001; Hughen et al., 1996; O'Brien et al., 1995). Climatic declines during 3200–3000 a BP have been documented in the high-resolution studies of GISP2 ice-cores from the Greenland ice cap, deep-sea cores from the North Atlantic, peat and lake sediments from the tropical Atlantic region, lake sediment and glacier advances from the Alpine region, and the Holocene flood frequency across the Central Alps (Bond et al., 2001; Haug et al., 2001; Hughen et al., 1996; Ivy-Dachs et al., 2009; Mayewski et al., 2004; O'Brien et al., 1995; Swierczynski et al., 2013; Wirth et al., 2013). Furthermore, the paleofloods at 3200–3000 a BP on the upper Yellow River were not unique events. For example, based on paleo-hydrological studies, extreme paleoflood events in the same period were identified in the upstream of the famous Hukou Falls in the middle Yellow River and in the Jinghe River valley, one of the tributaries in the middle Weihe River, China (Huang et al., 2012a, 2012c; Li et al., 2010). Therefore, it can be inferred that the paleoflood events occurring at the Jingyuan–Jingtai reach of the upper Yellow River gorges were the result of the regional hydrological system in response to abrupt climatic variability at approximately 3200–3000 a BP in the arid to semi-arid and sub-humid regions of China.

#### *Broader implications of the findings and paleoflood hydrology in a global context*

Conventional paleoflood hydrology focuses on general theories about floods and their frequencies in time and space. Although some extreme and rare flood data were collected, flood damages and hazards on the earth's surface do not lead to reduction (Baker, 2006). Recently, hydrologist, geologists, and geomorphologists have devoted themselves to addressing the practical mitigation problems. This has motivated the transition of paleoflood hydrology from conventional flood science to the practical application. These have ultimately led to the rapid development and improvement of quantitative computer models and methodology. Some new paleoflood hydrological approaches (e.g. Carivick, 2007; Huang et al., 2011, 2012a, 2012b, 2013; Miyamoto et al., 2006; Pelletier et al., 2005) have been used by flood engineers and flood experts to reconstruct the extreme paleoflood events (including the accurate recovery of magnitudes and frequency and return-period). The ages of the rare floods were dated based on dating techniques so that the floods that occurred during past millennia could be investigated and studied. The calculated flood data were used to implement a hazard assessment, to discover the realities of natural flood causation in a region, and to identify the zones that are hazardous to human development. This paper achieved integration of the gauged data, long-term historical and paleoflood records with paleo-hydrological studies from the upper Yellow River basin in China. The series of paleoflood data was used for flood frequency analysis using a method of adjusted moments for fitting the log Pearson type III distribution (US Water Resources Council, 1982). The work can be employed for safety investigations of dams and also to aid humankind in its anticipation of flood hazards and water-resource management.

The scientific research of paleoflood hydrology is carried out in the global context. Paleoflood data have now been documented over much of the world, especially in the United States (e.g. Greenbaum et al., 2001; Webb and Jarrett, 2002), Spain (e.g.

Benito et al., 2003; Thorndycraft et al., 2005), France (e.g. Sheffer et al., 2008), South Africa (e.g. Zawada, 1997, 2000; Zawada and Hattingh, 1994), India (e.g. Ely et al., 1996; Kale et al., 2000, 2003), and Australia (e.g. Gillieson et al., 1991; Wohl, 1992). These studies not only promoted the improvement of paleoflood hydrology but also showed that abrupt climate change and extreme events could well pose more of a hazard to human industry and activities than the mean climate phenomena predicted by global circulation models.

## Conclusion

Paleoflood methodological approaches were applied to a Holocene paleo-hydrological study in the Jingyuan–Jingtai reach on the upper Yellow River valley. During the fieldwork of paleoflood investigations, a bedset of SWD was identified at the JPC site in the upper Yellow River valley. The paleoflood peak stages were obtained from sedimentological evidence of floodwater elevations and the peak discharges were estimated between 12,750 and 16,310 m<sup>3</sup>/s using the step-backwater calculations with the HEC-RAS hydraulic model. The ages of paleoflood events were dated to have occurred between 3200 and 3000 a BP by OSL dating. The evidence from paleofloods indicates that extreme floods of a larger magnitude than any recorded in the instrumental and historical data series have occurred during the Holocene. In other words, paleoflood events recorded at the JPC site in the Jingyuan–Jingtai reach were the largest floods on the upper Yellow River basin during the late Holocene from 3200–3000 a BP to the present.

The flood sequence on a long timescale is of great importance in the analysis of flood frequency and magnitude, which is the basis of hydraulic engineering, managing river channels, and flood hazard mitigation. In addition, the long-term paleoflood records can also be used as valuable proxies that explain the individual extreme hydrological events in the hydrological regime responding to Holocene climatic variability. Based on a comparison with other proxies in the semi-arid and arid region of China and worldwide, the global climate was unstable and variable. Extreme floods are parts of climatic deterioration in the hydraulic system of the upper Yellow River. These achievements provide a reference for understanding the interactions between the hydrological system and climatic change in monsoonal regions of China.

## Acknowledgements

We thank the editors and anonymous reviewers for their valuable comments and constructive suggestions.

## Funding

This work was supported by the grant from the National Science Foundation of China (41471071) and the Innovation Fund of the Graduate Programs, SNNU (2015CX046).

## References

- Adamiec G and Aitken MJ (1998) Dose-rate conversion factors: Update. *Ancient TL* 16: 37–50.
- Baker VR (1987) Paleoflood hydrology and extreme flood events. *Journal of Hydrology* 96: 79–99.
- Baker VR (2006) Paleoflood hydrology in a global context. *Catena* 66: 161–168.
- Baker VR, Kochel RC, Patton PC et al. (1983) Paleohydrologic analysis of Holocene flood slack-water sediments. In: Collinson J and Lewin J (eds) *Modern and Ancient Fluvial Systems: Sedimentology and Processes* (Special Publication, vol. 6.). Gent: International Association of Sedimentologists, pp. 229–239.

- Banerjee D, Murray AS, Bøtter-Jensen L et al. (2001) Equivalent dose estimation using a single aliquot of polymineral fine grains. *Radiation Measurements* 33: 73–94.
- Benito G and Thorndycraft VR (2005) Paleoflood hydrology and its role in applied hydrological sciences. *Journal of Hydrology* 313: 3–15.
- Benito G, Lang M, Barriendos M et al. (2004) Use of systematic paleoflood and historical data for the improvement of flood risk estimation: Review of scientific methods. *Natural Hazards* 31: 623–643.
- Benito G, Sopena A, Sánchez-Moya Y et al. (2003) Paleoflood record of the Tanguis River (central Spain) during the Late Pleistocene and Holocene. *Quaternary Science Reviews* 22: 1737–1756.
- Bond G, Kromer B, Beer J et al. (2001) Persistent solar influence on North Atlantic climate during the Holocene. *Science* 294: 2130–2136.
- Bøtter-Jensen L and Duller GAT (1992) A new system for measuring optically stimulated luminescence from quartz samples. *International Journal of Radiation Applications and Instrumentation. Part D. Nuclear Tracks and Radiation Measurements* 20: 549–553.
- Carrivick JL (2007) Hydrodynamics and geomorphic work of Jokulhlaups (glacial outburst floods) from Kverkfjoll volcano, Iceland. *Hydrological Processes* 21: 725–740.
- Chen CTA, Lan HC, Lou JY et al. (2003) The dry Holocene megathermal in Inner Mongolia. *Paleogeography, Paleoclimatology, Paleoecology* 193: 181–200.
- COHMAP (1988) Climate changes of the last 18,000 years: Observations and model simulations. *Science* 241: 1043–1052.
- Ely LL and Baker VR (1985) Reconstructing paleoflood hydrology with slackwater deposits – Verde River, Arizona. *Physical Geography* 6: 103–126.
- Ely LL, Enzel Y, Baker VR et al. (1996) Changes in the magnitude and frequency of late Holocene monsoon floods on the Narmada River, central India. *Geological Society of America* 108: 1134–1148.
- Galbraith RF (1990) The radial plot: Graphical assessment of spread in ages. *Nuclear Tracks Radiation Measurements* 17: 207–214.
- Gao ZD, Li WJ, Li HR et al. (2002) The study on rainstorm and climatic change in the Yellow River basin. *Yellow River Water Conservancy Press*: 54–63 (in Chinese).
- Gillieson D, Smith DL, Greenaway M et al. (1991) Flood history of the Limestone ranges in the Kimberly region, Western Australia. *Applied Geography* 11: 105–123.
- Greenbaum N, Enzel Y and Schick AP (2001) Magnitude and frequency of paleofloods and historical floods in the Arava basin, Negev Desert, Israel. *Israel Journal of Earth Sciences* 50: 159–186.
- Grün R (2003) *The Age.exe Computer Program for the Calculation of Luminescence Dates*. Canberra: RSES.
- Haug GH, Hughen KA, Sigman DH et al. (2001) Southward migration of the intertropical convergence zone through the Holocene. *Science* 293: 1304–1308.
- Huang RH and Du ZC (2010) Evolution characteristics and trend of droughts and floods in China under the background of global warming. *Chinese Journal of Nature* 32(4): 187–195 (in Chinese with English abstract).
- Huang CC, Li XG, Pang JL et al. (2012c) Paleoflood sedimentological and hydrological studies on the Yongheguan reach in the middle Yellow River. *Acta Geographica Sinica* 67(11): 1493–1504 (in Chinese with English abstract).
- Huang CC, Pang JL, Su HX et al. (2009) The Ustic Isohumisol (Chernozem) distributed over the Chinese Loess Plateau: Modern soil or paleosol. *Geoderma* 150: 344–358.
- Huang CC, Pang JL, Zha XC et al. (2011) Prehistorical floods in the Guanzhong Basin in the Yellow River drainage area: A case study along the Qishuihe River Valley over the Zhouyuan Loess Tableland. *Sci sin Terrace* 41(11): 1685–1669 (in Chinese with English abstract).
- Huang CC, Pang JL, Zha XC et al. (2012a) Holocene Paleoflood events recorded by slackwater deposits along the Lower Jinghe River Valley, Middle Yellow River Basin, China. *Journal of Quaternary Science* 27(5): 485–493.
- Huang CC, Pang JL, Zha XC et al. (2012b) Sedimentary records of the extraordinary floods at the ending of the mid-Holocene Climatic Optimum along the upper Weihe River, China. *The Holocene* 22(6): 675–686.
- Huang CC, Pang JL, Zha XC et al. (2013) Extraordinary hydroclimatic events during the period AD 200–300 recorded by slackwater deposits in the upper Hanjiang River valley, China. *Palaeogeography, Palaeoclimatology, Palaeoecology* 374: 274–283.
- Hughen KA, Overpeck J, Peterson L et al. (1996) Rapid climate changes in the tropical Atlantic region during the last deglaciation. *Nature* 380: 51–54.
- Kale VS, Mishra S and Baker VR (2003) Sedimentary records of paleofloods in the bedrock gorges of the Tapi and Narmada Rivers, central India. *Current Science* 84: 1072–1079.
- Kale VS, Singhvi AK, Mishra PK et al. (2000) Sedimentary records and luminescence chronology of late Holocene paleofloods in the Luni River, Thar Desert, northwest India. *Catena* 40: 337–358.
- Kang LL, Leung LR, Liu C et al. (2015) Simulative study of the future climate and hydrological change over the Yellow River basin. *Acta Meteorological Sinica* 73(2): 382–393 (in Chinese with English abstract).
- Kochel RC and Baker VR (1982) Paleoflood hydrology. *Science* 215: 353–361.
- La CL, Hao YH and Hou TY (2013) The analysis on 2012 flood in the Lanzhou reaches of Yellow River. *Gansu Water Resources and Hydropower Technology* 49(4): 3–4 (in Chinese with English abstract).
- Lan YC, Lin S, Wen J et al. (2007) Studies on atmospheric circulation anomaly of flood period and prefreshet periods in the highest and lowest flow years in the upper Yellow River. *Plateau Meteorology* 26(5): 1052–1058 (in Chinese with English abstract).
- Liu TS and Wang LS (2002) Research on geological environment evolution and collapse and landside occurred in Yellow River. *Geotectonica et Metallogenia* 26: 203–206 (in Chinese with English abstract).
- Li XG (2013) The progress of paleoflood researches in the Yellow River. *Journal of Shangluo College* 27(2): 57–63 (in Chinese with English abstract).
- Li XG, Huang CC, Pang JL et al. (2010) Hydrological studies of the Holocene paleoflood in the Hukou reach of the Yellow River. *Acta Geographica Sinica* 65(11): 1371–1380 (in Chinese with English abstract).
- Mayewski PA, Rohling EE, Stager JC et al. (2004) Holocene climate variability. *Quaternary Research* 62: 243–255.
- Milly PCD, Betancourt J, Falkenmark M et al. (2008) Stationarity is dead: whither water management. *Science* 319: 573–574.
- Miyamoto H, Itoh K, Komatsu G et al. (2006) Numerical simulations of large-scale cataclysmic floodwater: A simple depth-averaged model and an illustrative application. *Geomorphology* 76: 179–192.
- Murray AS and Wintle AG (2000) Luminescence dating of quartz using an improved single-aliquot regenerative-dose protocol. *Radiation Measurements* 32: 57–73.

- O'Brien SR, Mayewski PA, Meeker LD et al. (1995) Complexity of Holocene climate as reconstructed from a Greenland ice-core. *Science* 270: 1962–1964.
- O'Connor JE and Webb RH (1988) Hydraulic modelling for paleoflood analysis. In: Baker VR, Kochel RC and Patton PC (eds) *Flood Geomorphology*. New York: John Wiley & Sons, pp. 393–402.
- Pelletier JD, Mayer L, Pearthree PA et al. (2005) An integrated approach to alluvial-fan flood hazard assessment with numerical modeling, field mapping, and remote sensing. *Geological Society of America Bulletin* 117: 1167–1180.
- Peng Y, Xiao J, Nakamura T et al. (2005) Holocene East Asian monsoonal precipitation pattern revealed by grain-size distribution of core sediments of the Daihai Lake in Inner-Mongolia of North-central China. *Earth and Planetary Science Letters* 233: 467–479.
- Ran LS, Wang SL, Fan XL et al. (2009) Analysis on the relation about the waterpower geometry of the upper Yellow River. *Yellow River* 31(6): 38–41 (in Chinese).
- Ren LX and Feng YN (2008) Annual runoff variation of the Yellow River in Lanzhou station at different times. *Science and Technology Innovation Herald* 24: 62–64 (in Chinese with English abstract).
- Rittenour TM, Goble RJ and Blum MD (2003) An optical age chronology of Late Pleistocene fluvial deposits in the northern lower Mississippi valley. *Quaternary Science Review* 22: 1105–1110.
- Sheffer NA, Rico M, Enzel Y et al. (2008) The paleoflood record of the Gardon River, France: A comparison with the extreme 2002 flood event. *Geomorphology* 98: 71–83.
- Shi YF, Kong ZC and Wang SM (1992) The important climatic fluctuations and events in China during the Holocene megathernal. *Science in China* 22: 1300–1308 (in Chinese).
- Sridhar A (2007) A mid-late Holocene flood record from the alluvial reach of the Mahi River, Western India. *Catena* 70: 330–339.
- Støren EN, Kolstad EW and Paasche Ø (2012) Linking past flood frequencies in Norway to regional atmospheric circulation anomalies. *Journal of Quaternary Science* 27: 71–80.
- Sun JZ and Zhao JB (1991) *Quaternary of Loess Plateau in China*. Beijing: Science Press, pp. 186–205 (in Chinese).
- Swierczynski T, Lauterbach S, Dulski P et al. (2013) Mid- to late Holocene flood frequency changes in the northeastern Alps as recorded in varved sediments of Lake Mondsee (Upper Austria). *Quaternary Science Reviews* 80: 78–90.
- Thomas PJ, Jain M, Juyal N et al. (2005) Comparison of sin-grain and small-aliquot OSL dose estimate in <3000 years old river sediments from South India. *Radiation Measurements* 39: 457–469.
- Thorndycraft VR, Benito G, Rico M et al. (2005) A long-term flood discharge record derived from slack-water flood deposits of the Llobregat River, NE Spain. *Journal of Hydrology* 313: 16–31.
- US Army Corps of Engineers Hydraulic Engineering Center (2010) *HEC-RAS River Analysis System: Hydraulic Reference Manual*. Davis, CA: US Army Corps of Engineers.
- US Water Resources Council (1982) *Guidelines for Determining Flood Flow Frequency* (Bulletin, vol. 17B of the Hydrology Committee), [http://water.usgs.gov/osw/bulletin17b/dl\\_flow.pdf](http://water.usgs.gov/osw/bulletin17b/dl_flow.pdf).
- Webb RH and Jarrett RD (2002) One-dimensional estimation techniques for discharges of paleofloods and historical floods. In: House PK, Webb RH, Baker VR et al. (eds) *Ancient Floods, Modern Hazards: Principles and Applications of Paleoflood Hydrology. Water Resources Monograph*, vol. 5. John Wiley & Sons, pp. 111–125.
- Wirth SB, Glur L, Gilli A et al. (2013) Holocene flood frequency across the Central Alps – Solar forcing and evidence for variations in North Atlantic atmospheric circulation Original Research Article. *Quaternary Science Reviews* 80: 112–128.
- Wohl EE (1992) Bedrock benches and boulder bars: Floods in the Burdekin Gorge of Australia. *Geological Society of America Bulletin* 104: 770–778.
- Xiao JL, Chang ZG, Wen RL et al. (2009) Holocene weak monsoon intervals indicated by low lake levels at Hulun Lake in the monsoonal margin region of northeastern Inner Mongolia, China. *The Holocene* 19: 899–908.
- Xiao JL, Xu QH, Nakamura T et al. (2004) Holocene vegetation variation in the Daihai Lake region of north-central China: A direct indication of the Asian monsoon climatic history. *Quaternary Science Review* 23: 1669–1679.
- Xie BJ, Cheng J and Tian MZ (2011) Effects of Qinghai-Tibet plateau uplift on climate and Eco-environment during the Quaternary: A case analysis for the central section of Gangdise, Tibet. *Geology and Exploration* 47:121–132.
- Yang DY, Yu G, Xie YB et al. (2000) Sedimentary records of large Holocene floods from the middle reach of the Yellow River, China. *Geomorphology* 33: 73–88.
- Zawada PK (1997) Paleoflood hydrology: Method and application in flood-prone southern Africa. *South Africa Journal of Science* 93: 111–132.
- Zawada PK (2000) Paleoflood hydrology of selected South African rivers. *South African Geological Survey Memoir* 87: 173.
- Zawada P and Hattingh J (1994) Studies on the paleoflood hydrology of South African rivers. *South African Journal of Science* 90: 567–568.
- Zhang JF, Zhou LP and Yue SY (2003) Dating fluvial sediments by optically stimulated luminescence: Selection of equivalent doses for age calculation. *Quaternary Science Reviews* 22: 1123–1129.
- Zhang HP, Zhang PZ, Wu QL et al. (2008) Characteristic of the Huanghe River longitudinal profiles around Xunhua-Guizhou area (Ne Tibet) and their tectonic significance. *Quaternary Sciences* 28(2): 299–307 (in Chinese with English abstract).